

trans*-Bis[(*S*)-(-)-2-aminomethyl-1-ethylpyrrolidine- κ^2 N]palladium(II) dichloride methanol trisolvate*Matthew D. Jones, Filipe A. Almeida Paz, John E. Davies, Brian F. G. Johnson* and Jacek Klinowski**

Department of Chemistry, University of Cambridge, Lensfield Road, Cambridge CB2 1EW, England

Correspondence e-mail: bfgj1@cam.ac.uk

Key indicators

Single-crystal X-ray study

 $T = 180$ KMean $\sigma(\text{C}-\text{C}) = 0.005$ Å

Disorder in solvent or counterion

 R factor = 0.036 wR factor = 0.075

Data-to-parameter ratio = 21.9

For details of how these key indicators were automatically derived from the article, see <http://journals.iucr.org/e>.

The crystal structure of the title compound, $[\text{Pd}(\text{C}_7\text{H}_{16}\text{N}_2)_2]\text{Cl}_2 \cdot 3\text{CH}_3\text{OH}$, has been determined at 180 (2) K in the non-centrosymmetric space group $P2_12_12_1$. The structure contains only one crystallographically unique Pd metal centre, showing a slightly distorted square-planar geometry, in which the two chiral (*S*)-(-)-2-aminomethyl-1-ethylpyrrolidine diamines are coordinated with a *trans* configuration in order to minimize the steric interaction between neighbouring substituent ethyl groups. $[\text{Pd}(\text{C}_7\text{H}_{16}\text{N}_2)_2]^{2+}$ complex cations are strongly hydrogen-bonded to the Cl^- anions and methanol molecules, forming supramolecular tapes running along the *a* axis.

Received 6 October 2003

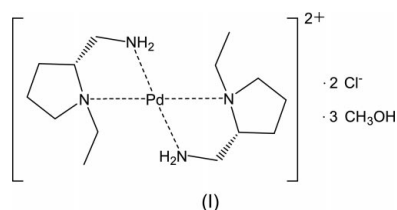
Accepted 13 October 2003

Online 23 October 2003

Comment

Asymmetric catalysis, defined as the ability to form one enantiomer selectively in preference to the other in the presence of an appropriate catalyst, is one of the most important advances in modern industrial chemistry. To date, the majority of organic ligands used in asymmetric catalysts with late transition metals have been based on phosphines, with only a very few reports of *N*-donor ligands bound to Rh or Pd metal centres (Noyori, 2002; Fache *et al.*, 2000; Tommasino *et al.*, 1999). We have recently explored the use of diamines, which can lead to chiral catalysts with direct applications in asymmetric hydrogenation processes (Jones, Raja *et al.*, 2003; Jones, Almeida Paz *et al.*, 2003*a,b*; Rouzaud *et al.*, 2003).

Attempts to synthesize Pd-based catalysts have used $[\text{PdCl}_2(\text{PhCN})_2]$ as the Pd precursor, in which the weakly bound benzonitrile ligands could easily be displaced by diamines (denoted N–N) in the presence of a suitable solvent (*e.g.* CH_2Cl_2) to form the neutral catalytic species $[\text{PdCl}_2(\text{N}-\text{N})]$ (Sauthier *et al.*, 2000; Newman *et al.*, 1999; Satake *et al.*, 1999). Surprisingly, when the chiral diamine ligand (*S*)-(-)-2-aminomethyl-1-ethylpyrrolidine (amepd) was used (see Scheme), it displaced not only the PhCN species but also the Cl ligands, forming a $[\text{Pd}(\text{amepd})_2]^{2+}$ cationic palladium complex as its solvated chloride salt, (I), the crystal structure of which we report here.



(I)

1-ethylpyrrolidine might, in theory, lead to two possible isomers, *cis* and *trans*. However, only one isomer is observed in (I), with the two coordinated diamine molecules having equivalent *N*-donor atoms *trans* to each other (Fig. 1). The *trans* arrangement is presumably preferred to the *cis* arrangement because it minimizes the steric repulsion between the ethyl substituent groups from adjacent coordinated diamines (Fig. 1).

As has been observed for related complexes, the Pd metal centre in (I) (with an electron count of 16) is found in a slightly distorted square-planar geometry (Fig. 1), the Pd–N and N–Pd–N distances and angles being consistent with those found in the literature (Table 1; Bruno *et al.*, 2002; Albinati *et al.*, 1991).

Classical strong (N–H···O) and very strong (*X*–H···Cl[−], where *X* is N or O) cooperative hydrogen bonds in (I) link together neighbouring [Pd(amepd)₂]²⁺ complexes (Table 2), leading to the formation of an *R*₇⁴(18) graph-set motif (Fig. 2), which alternates in a zigzag fashion along the *a* axis of the unit cell (Fig. 3), leading to the formation of hydrogen-bonded supramolecular tapes of (I). Individual tapes, related by the 2₁ screw axis, pack in an [ABAB...] fashion along the *b* axis (two layers per unit-cell repeat; Fig. 4).

Experimental

All chemicals were purchased from Aldrich and used without further purification. Solvents were dried and degassed using appropriate methods. Standard Schlenk line techniques were also employed. [PdCl₂(PhCN)₂] (140 mg, 0.036 mmol) was dissolved in tetrahydrofuran (*ca* 10 ml), followed by the addition of (*S*)-(−)-2-aminomethyl-1-ethylpyrrolidine (0.05 ml, 0.36 mmol). The resulting solution was stirred at ambient temperature for 1 h. A white precipitate was filtered, washed with diethyl ether (2 × *ca* 20 ml) and dried *in vacuo* to give a white microcrystalline powder. Crystals of (I) suitable for X-ray diffraction analysis were obtained by recrystallization from a CH₂Cl₂–Et₂O–MeOH solution (5:1:1). Analysis calculated for C₁₄H₃₂N₂PdCl₂: C 38.80, H 7.39, N 12.93%; found: C 37.56, H 7.28,

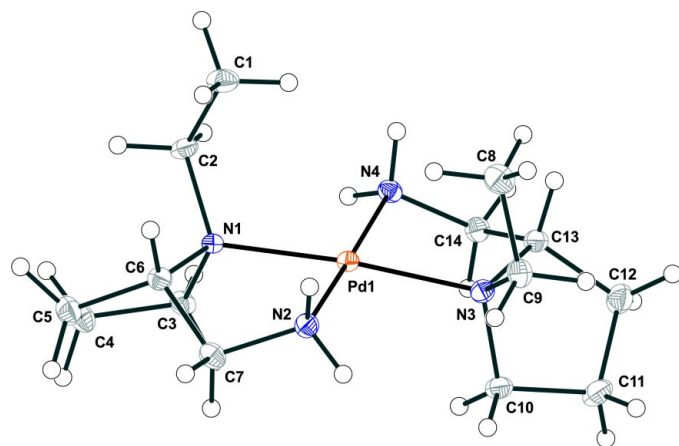


Figure 1
A view of the [Pd(C₇H₁₆N₂)₂]²⁺ complex cation in (I), showing the labelling scheme for all non-H atoms. Displacement ellipsoids are drawn at the 30% probability level and H atoms are shown as small spheres. The Cl[−] anions and the methanol molecules have been omitted for clarity.

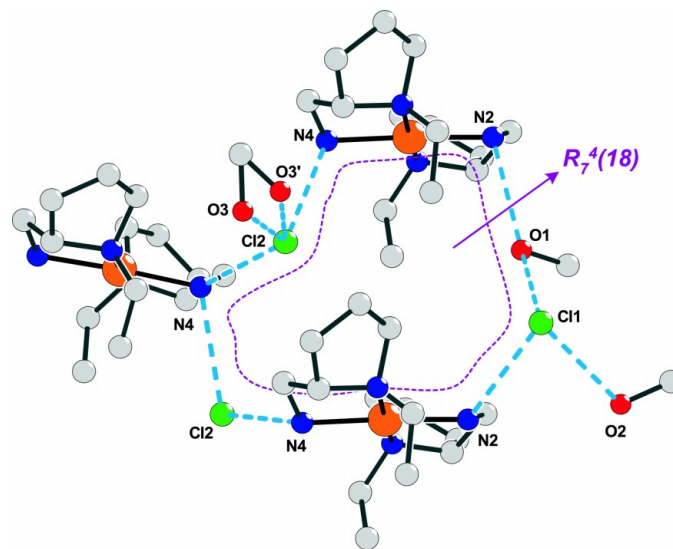


Figure 2
A view of the *R*₇⁴(18) graph-set motif formed by the hydrogen bonds linking neighbouring [Pd(C₇H₁₆N₂)₂]²⁺ complex cations. For hydrogen-bond details see Table 2. H atoms have been omitted for clarity.

N 12.31%. Spectroscopic analysis: ¹H NMR (CD₃OD, δ, p.p.m.): 1.64 (*t*, *J* = 7 Hz, 3H), 1.85–2.30 (*m*, CH₂, 4H), 2.65–3.65 (*m*, NCH, NCH₂, 7H); ¹³C NMR (CD₃OD, δ, p.p.m.): 12.3 (CH₃), 22.1 (CH₂), 23.5 (CH₂), 53.8 (NCH₂), 59.4 (NCH₂), 69.5 (NCH); positive ESI = 181 (*M*²⁺, 100%).

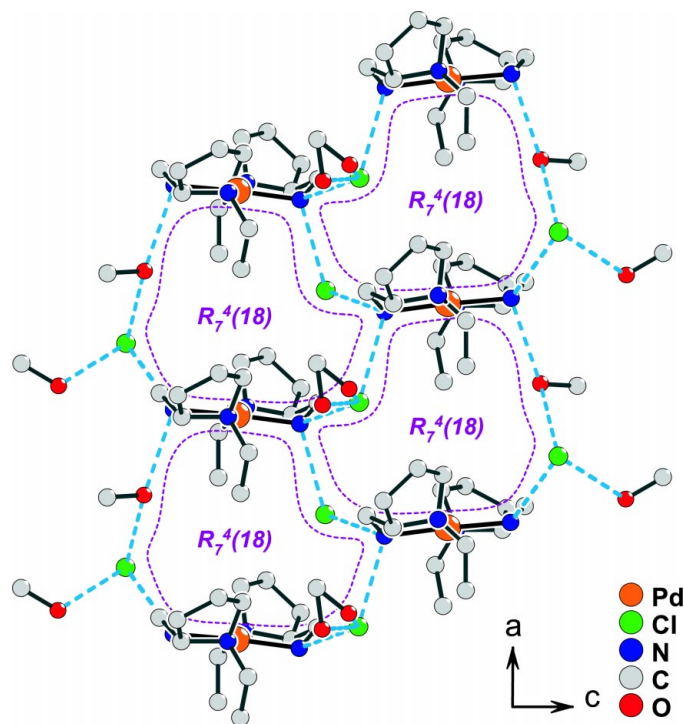


Figure 3
The supramolecular tape of (I) formed by the zigzag alternation of the *R*₇⁴(18) graph-set motif along the *a* axis of the unit cell. H atoms have been omitted for clarity.

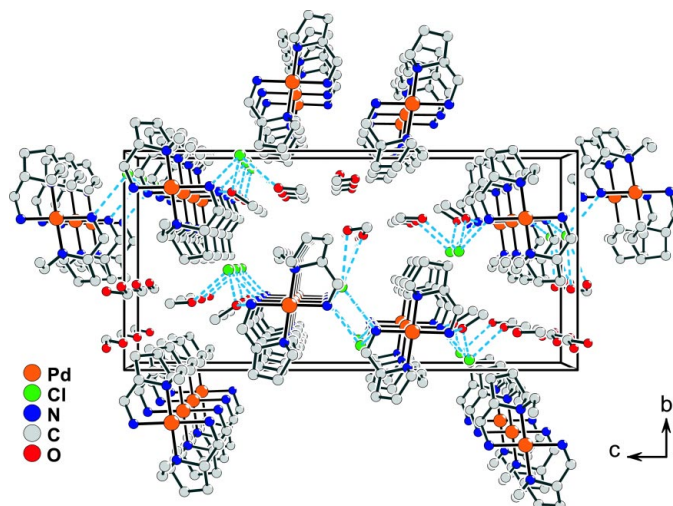


Figure 4
Perspective view of (I) along the a axis. Hydrogen bonds ($N-H \cdots O$ and $X-H \cdots Cl^-$, where X is N or O) are drawn as blue dashed lines (see Table 2 for hydrogen-bonding geometry). H atoms have been omitted for clarity.

Crystal data

$[Pd(C_7H_{16}N_2)_2]Cl_2 \cdot 3CH_4O$
 $M_r = 529.86$
 Orthorhombic, $P2_12_12_1$
 $a = 7.3092$ (1) Å
 $b = 12.9075$ (2) Å
 $c = 26.3277$ (6) Å
 $V = 2483.85$ (8) Å³
 $Z = 4$
 $D_x = 1.417$ Mg m⁻³

Mo $K\alpha$ radiation
 Cell parameters from 14 842 reflections
 $\theta = 1.0$ – 27.5°
 $\mu = 0.99$ mm⁻¹
 $T = 180$ (2) K
 Block, yellow
 $0.23 \times 0.10 \times 0.10$ mm

Data collection

Nonius Kappa CCD area-detector diffractometer
 Thin-slice ω and φ scans
 Absorption correction: multi-scan (SORTAV; Blessing, 1995)
 $T_{min} = 0.843$, $T_{max} = 0.906$
 14 487 measured reflections

5324 independent reflections
 4721 reflections with $I > 2\sigma(I)$
 $R_{int} = 0.046$
 $\theta_{max} = 27.5^\circ$
 $h = -9 \rightarrow 9$
 $k = -16 \rightarrow 16$
 $l = -29 \rightarrow 34$

Refinement

Refinement on F^2
 $R[F^2 > 2\sigma(F^2)] = 0.036$
 $wR(F^2) = 0.075$
 $S = 1.01$
 5324 reflections
 243 parameters
 H-atom parameters constrained

$w = 1/[\sigma^2(F_o^2) + (0.0286P)^2 + 1.4529P]$
 where $P = (F_o^2 + 2F_c^2)/3$
 $(\Delta/\sigma)_{max} = 0.002$
 $\Delta\rho_{max} = 0.52$ e Å⁻³
 $\Delta\rho_{min} = -1.10$ e Å⁻³
 Absolute structure: Flack (1983), 2149 Friedel pairs
 Flack parameter = -0.02 (3)

Table 1

Selected geometric parameters (Å, °).

Pd1–N2	2.041 (3)	Pd1–N1	2.056 (3)
Pd1–N4	2.044 (3)	Pd1–N3	2.059 (3)
N2–Pd1–N4	177.17 (11)	N2–Pd1–N3	96.33 (12)
N2–Pd1–N1	83.80 (12)	N4–Pd1–N3	83.80 (12)
N4–Pd1–N1	96.36 (12)	N1–Pd1–N3	174.09 (12)

Table 2

Hydrogen-bonding geometry (Å, °).

$D-H \cdots A$	$D-H$	$H \cdots A$	$D \cdots A$	$D-H \cdots A$
N2–H2A ⁱ ···Cl1 ⁱ	0.92	2.35	3.225 (3)	159
N2–H2B ⁱⁱ ···O1 ⁱⁱ	0.92	2.07	2.949 (4)	160
N4–H4A ⁱⁱⁱ ···Cl2 ⁱⁱⁱ	0.92	2.37	3.240 (3)	158
N4–H4B ⁱⁱⁱ ···Cl2	0.92	2.36	3.222 (3)	156
O1–H1 ^{iv} ···Cl1	0.84	2.31	3.127 (3)	166
O2–H2 ^{iv} ···Cl1	0.84	2.37	3.205 (4)	176
O3–H3 ^{iv} ···Cl2 ^{iv}	0.84	2.40	3.146 (8)	148
O3'–H3'···Cl2 ^{iv}	0.84	2.50	3.224 (8)	145

Symmetry codes: (i) $1 - x, \frac{1}{2} + y, \frac{1}{2} - z$; (ii) $2 - x, \frac{1}{2} + y, \frac{1}{2} - z$; (iii) $x - \frac{1}{2}, \frac{3}{2} - y, -z$; (iv) $x, y, 1 + z$.

All H atoms were placed at calculated positions and made to ride during subsequent refinement, with $U_{iso}(H) = xU_{eq}(C \text{ or } N)$, where $x = 1.5$ for the methyl groups of the $[Pd(C_7H_{16}N_2)_2]^{2+}$ cation and $x = 1.2$ for others. H atoms of the –OH groups of the methanol molecules were also placed in calculated positions, to give the best hydrogen-bonding interactions. One methanol molecule was found to be disordered and was modelled with fixed 50% occupancy factors for each position. C and O atoms of this disordered methanol molecule were refined with a common isotropic displacement parameter. The last difference Fourier map synthesis showed a residual electron density with the highest peak located at 1.43 Å from H1B, and the deepest hole located at 0.84 Å from Pd1.

Data collection: COLLECT (Nonius, 1998); cell refinement: HKL SCALEPACK (Otwinowski & Minor, 1997); data reduction: HKL DENZO (Otwinowski & Minor, 1997) and SCALEPACK; program(s) used to solve structure: SIR92 (Altomare *et al.*, 1994); program(s) used to refine structure: SHELXTL (Bruker, 2001); molecular graphics: SHELXTL; software used to prepare material for publication: SHELXTL.

We thank the EPSRC for a studentship to MDJ and for their general financial support, and ICI and the Newton Trust for financial support. We are also grateful to the Portuguese Foundation for Science and Technology (FCT) for financial support through PhD scholarship No. SFRH/BD/3024/2000 for FAAP.

References

- Albinati, A., Kunz, R., Ammann, C. & Pregosin, P. S. (1991). *Organometallics*, **10**, 1800–1806.
 Altomare, A., Cascarano, G., Giacovazzo, C., Guagliardi, A., Burla, M. C., Polidori, G. & Camalli, M. (1994). *J. Appl. Cryst.* **27**, 435.
 Blessing, R. H. (1995). *Acta Cryst.* **A51**, 33–58.
 Bruno, G., Lanza, S., Nicolo, F., Tresoldi, G. & Rosace, G. (2002). *Acta Cryst.* **C58**, m316–m318.
 Bruker (2001). *SHELXTL*. Version 6.12. Bruker AXS Inc., Madison, Wisconsin, USA.
 Fache, F., Schultze, E., Tommasino, M. L. & Lemaire, M. (2000). *Chem. Rev.* **100**, 2159–2231.
 Flack, H. D. (1983). *Acta Cryst.* **A39**, 876–881.
 Jones, M. D., Almeida Paz, F. A., Davies, J. E. & Johnson, B. F. G. (2003a). *Acta Cryst.* **E59**, m6–m7.
 Jones, M. D., Almeida Paz, F. A., Davies, J. E. & Johnson, B. F. G. (2003b). *Acta Cryst.* **E59**, m105–m107.
 Jones, M. D., Raja, R., Thomas, J. M., Johnson, B. F. G., Lewis, D. W., Rouzaud, J. & Harris, K. D. M. (2003). *Angew. Chem. Int. Ed.* **42**, 4326–4331.
 Newman, P. D., Hursthouse, M. B. & Malik, K. M. A. (1999). *J. Chem. Soc. Dalton Trans.* pp. 599–606.
 Nonius (1998). *COLLECT*. Nonius BV, Delft, The Netherlands.
 Noyori, R. (2002). *Angew. Chem. Int. Ed.* **41**, 2008–2022.

- Otwinowski, Z. & Minor, W. (1997). *Methods in Enzymology*, Vol. 276, *Macromolecular Crystallography*, Part A, edited by C. W. Carter Jr & R. M. Sweet, pp. 307–326. New York: Academic Press.
- Tommasino, M. L., Thomazeau, C., Touchard, F. & Lemaire, M. (1999). *Tetrahedron. Asymm.* **10**, 1813–1819.
- Rouzaud, J., Jones, M. D., Raja, R., Johnson, B. F. G., Thomas, J. M. & Duer, M. J. (2003). *Helv. Chim. Acta*, **86**, 1753–1759.
- Satake, A., Koshino, H. & Nakata, T. (1999). *Organometallics*, **18**, 5108–5111.
- Sauthier, M., Fornies-Camer, J. F., Toupet, L. & Reau, R. (2000). *Organometallics*, **19**, 553–562.